J Mater Sci (2006) 41:4604–4610
DOI 10.1007/s10853-006-0328-9

Micro-mechanical theory of macroscopic stress-corrosion cracking in unidirectional GFRP

H. Sekine · P. W. R. Beaumont

Received: 16 August 2004 / Accepted: 28 September 2005 / Published online: 6 June 2006

Abstract A micro-mechanical theory of macroscopic stress-corrosion cracking in a unidirectional glass fibre-reinforced polymer composite is proposed. It is based on the premise that under tensile loading, the time-dependent failure of the composite is controlled by the initiation and growth of a crack from a pre-existing inherent surface flaw in a glass fibre. A physical model is constructed and an equation is derived for the macroscopic crack growth rate as a function of the apparent crack tip stress intensity factor for mode I. Emphasis is placed on the significance of the size of inherent surface flaw and the existence of matrix crack bridging in the crack wake. There exists a threshold value of the stress intensity factor below which matrix cracking does not occur. For the limiting case, where the glass fibre is free of inherent surface flaws and matrix crack bridging is negligible, the relationship between the macroscopic crack growth rate and the apparent crack tip stress intensity factor is given by a simple power law to the power of two.

Introduction

Glass fibre-reinforced polymer composites (GFRP) are widely used in the construction of pipes and tanks containing acidic solutions. In most cases, where stresses are low and the acid is sufficiently dilute, these applications are successful. However, the literature is full of examples of stress-corrosion cracking of GFRP, when the stress and environmental conditions have been severe.

For example, Hogg and Hull [1], Noble et al. [2] and Price and Hull [3, 4] observed stress-corrosion cracking in glass fibres in a GFRP by scanning electron microscopy(SEM). Post mortem evidence of broken glass fibres indicated a two-stage fracture process: (1) a ''slow'' (meaning time-dependent) fracture of a portion of the glass fibre, whose surface is smooth, followed by (2) a ''fast'' fracture. The fine markings on the smooth portion of fracture surface could be traced back to an inherent surface flaw in the glass fibre. Once the glass fibre had completely failed, the crack extended into the surrounding polymer matrix (Fig. 1).

Interesting material behaviour which is frequently dynamic, with time-dependent characteristics, originates usually from a kinetic process, diffusion or the rate of a chemical reaction, all of which, but not always, contain an empirical component. In an engineering context, a first attempt at modelling this behaviour of stress-corrosion cracking in a GFRP would be to describe concisely a body of crack growth rate data as a function of the crack tip stress intensity factor using a fracture mechanics model [3–7]. But a better model, however, would be one that captures the essential physics of the engineering problem of fracture. Having identified the dominant microscopic processes responsible for stress-corrosion cracking in this instance, we then model them using the tools of micro-mechanics and our understanding of the theory of defects, and of reaction rates. The model would encapsulate the physics of the fracture processes

H. Sekine (✉)
Department of Aerospace Engineering, Tohoku University, Aoba-yama 6-6-01, Aoba-ku, Sendai 980-8579, Japan
e-mail: sekine@plum.mech.tohoku.ac.jp

P. W. R. Beaumont
Department of Engineering, University of Cambridge, Trumpington Street, Cambridge CB2 1PZ, UK

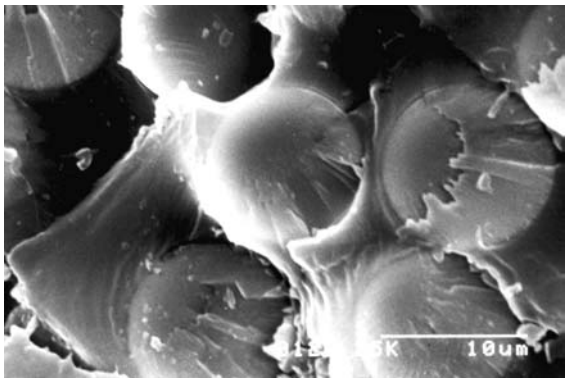

Fig. 1 Scanning electron micrograph of fracture surfaces of glass fibre

induced by a chemically active environment. It would illuminate the basic principles that underline the key elements of the stress-corrosion process. The micro-mechanical model would establish a physical framework within which empirical descriptions of the behaviour of some of the intrinsic and extrinsic variables can be attached. We begin with a simple picture or representation of the actual thing that a stress-corrosion crack initiates at a pre-existing inherent surface flaw in a glass fibre, propagates stably perpendicular to the fibre direction with time and finally leads to unstable fracture of the fibre (Fig. 2).

Micro-mechanical theory of stress-corrosion cracking

In bulk glass, the stable crack growth rate due to stress-corrosion cracking $\mathrm{d}a/\mathrm{d}t$ is given in the following form [10]

$$\frac{\mathrm{d}a}{\mathrm{d}t} = v \exp\left(-\frac{\Delta Q - \alpha K_{\mathrm{I}}}{RT}\right). \tag{1}$$

In this Arrhenius equation, ΔQ is the activation energy of the chemically activated process, K_{I} is the crack tip stress intensity factor for mode I, R is the gas constant, T is absolute temperature, and v and α are empirical constants. It should be noted that the activation energy ΔQ can sometimes be predicted from molecular models, but the value of the pre-exponential v and the constant α more often than not elude current modelling methods; they must be inserted empirically.

Sekine et al. [11] carried out a numerical simulation of the growth of a stress-corrosion crack in a glass fibre in a GFRP. This work showed that the shape of the crack front within the glass fibre can be approximated as a circular arc of radius r equal to the fibre radius r_{f} (Fig. 3). The average crack growth rate due to stress-corrosion of a glass fibre can be written from Eq. 1 as

$$\frac{1}{2r_{\mathrm{f}}\theta}\frac{\mathrm{d}Y}{\mathrm{d}t} = v \exp\left(-\frac{\Delta Q - \alpha K_{\mathrm{I}}}{RT}\right) \tag{2}$$

where Y is the area of the stress-corrosion crack in the glass fibre, θ is half the angle which is made by two fibre radii on the edges of the stress-corrosion crack, see Fig. 3, and t is time. In Eq. 2, K_{I} should be interpreted as the average value of the crack tip stress intensity factor along the crack front. Since the crack tip stress intensity factor is constant more or less over a large part of central portion of the circular crack front [11], we will represent K_{I} by the crack tip stress intensity factor at the maximum depth of the stress-corrosion crack [12]:

$$K_{\mathrm{I}} = \sigma_{\mathrm{f}} F(\theta)\sqrt{2\pi r_{\mathrm{f}}} \tag{3}$$

where σ_{f} is the tensile stress acting on the glass fibre and $F(\theta)$ is written as

$$\begin{aligned} F(\theta) = \sqrt{1-\cos\theta}\{&1.12 - 3.40(1-\cos\theta) \\ &+ 13.87(1-\cos\theta)^2 - 14.37(1-\cos\theta)^3\}. \end{aligned} \tag{4}$$

Consider the relationship between the tensile stress acting on a glass fibre ahead of the macroscopic stress-corrosion crack tip and the apparent crack tip stress intensity factor for mode I. When the glass fibres in a unidirectional GFRP are assumed to be distributed in doubly periodic array shown in Fig. 4, the distance D

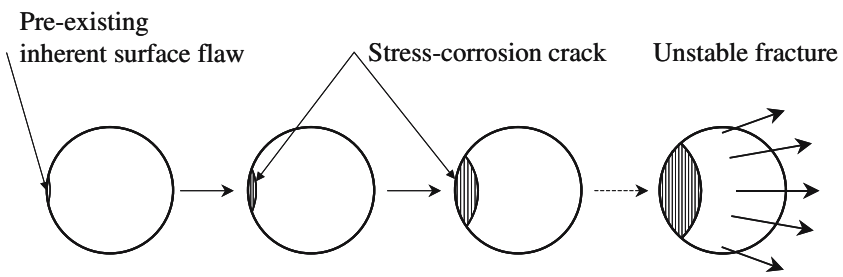

Fig. 2 Sekine–Miyanaga–Beaumont model [8, 9] of stress-corrosion crack growth in a glass fibre in a unidirectional GFRP

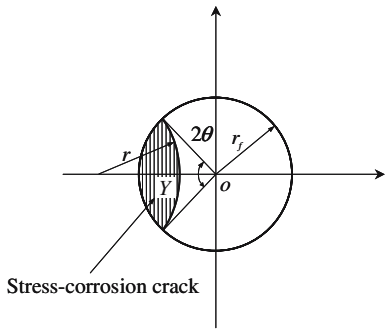

Fig. 3 Shape of stress-corrosion crack in a glass fibre

between the neighbouring rows of glass fibre is given by

$$D = c\sqrt{\frac{\pi}{V_{\mathrm{f}}}}r_{\mathrm{f}} \tag{5}$$

where

$$c = \begin{cases} 1 & \text{for square array of fibre} \\ \frac{1}{\sqrt{2}} = 0.707 & \text{for face-centred square array of fibre} \\ \sqrt{\frac{3^{1/2}}{2}} = 0.931 & \text{for face-centred hexagonal array of fibre} \end{cases} \tag{6}$$

and V_{f} is the volume fraction of glass fibre. Now, let us obtain the average tensile stress over the distance D just ahead of the macroscopic stress-corrosion crack tip. Since the unidirectional GFRP is macroscopically orthotropic, the macroscopic tensile stress in the fibre direction σ_y is characterized at the macroscopic crack tip by [13]

$$\sigma_y = \frac{K_{\mathrm{I}}^*}{\sqrt{2\pi x}} \tag{7}$$

where K_{I}^* is the apparent crack tip stress intensity factor for mode I and x is the rectangular coordinate axis whose origin is located at the macroscopic crack tip, see Fig. 4. Then, the average tensile stress over the distance D just ahead of the macroscopic stress-corrosion crack tip is given by

$$\tilde{\sigma}_y = \frac{1}{D}\int_0^D \frac{K_{\mathrm{I}}^*}{\sqrt{2\pi x}}\,\mathrm{d}x = K_{\mathrm{I}}^*\sqrt{\frac{2}{\pi D}}. \tag{8}$$

On the other hand, since the tensile stress ahead of the macroscopic stress-corrosion crack tip is supported by the glass fibre and matrix, the average tensile stress $\tilde{\sigma}_y$ is approximately estimated by

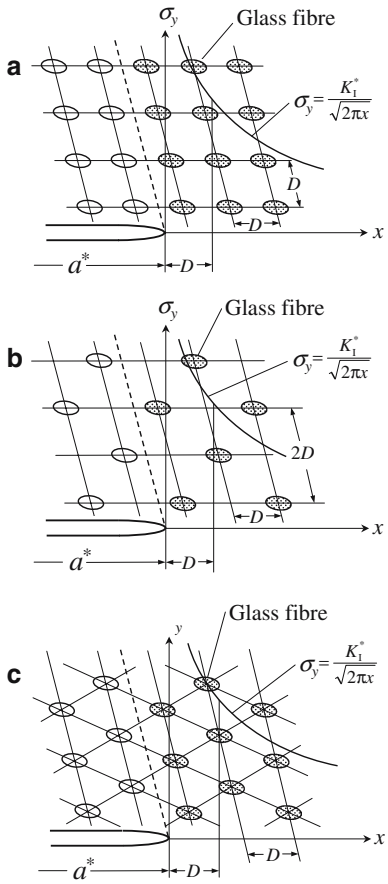

Fig. 4 Glass fibres distributed in doubly periodic array and macroscopic tensile stress distribution ahead of the macroscopic stress-corrosion crack tip

$$\tilde{\sigma}_y = \left\{V_{\mathrm{f}} + \frac{(1-V_{\mathrm{f}})E_{\mathrm{m}}}{E_{\mathrm{f}}}\right\}\sigma_{\mathrm{f}} \tag{9}$$

where E_{f} and E_{m} denote the Young's moduli of glass fibre and matrix, respectively.

In view of Eqs. 8 and 9, the relationship between the tensile stress acting on the glass fibre ahead of the macroscopic stress-corrosion crack tip σ_{f} and the apparent crack tip stress intensity factor K_{I}^* is given by

$$\sigma_{\mathrm{f}} = \beta K_{\mathrm{I}}^* \tag{10}$$

where

$$\beta = \frac{E_{\mathrm{f}}}{V_{\mathrm{f}}E_{\mathrm{f}} + (1-V_{\mathrm{f}})E_{\mathrm{m}}}\sqrt{\frac{2}{\pi D}}. \tag{11}$$

When tougher and more ductile polymer is used as a matrix, matrix crack bridging shown schematically in Fig. 5 may occur in the wake of the propagating macroscopic stress-corrosion crack in the unidirectional GFRP. Such mechanism reduces the apparent crack tip stress intensity factor K_{I}^*. Then, we obtain

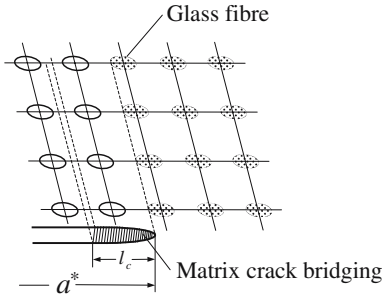

Fig. 5 Matrix crack bridging in the wake of the propagating macroscopic stress-corrosion crack. The direct observation of the matrix crack bridging in a GFRP has not been reported yet

$$K_{\mathrm{I}}^{*} = K_{Ia}^{*} + K_{Ib}^{*} \tag{12}$$

where K_{Ia}^{*} and K_{Ib}^{*} are the apparent crack tip stress intensity factors due to an applied load and matrix crack bridging, respectively.

In this section, the tensile characteristic of bridging polymer, i.e. fibrils of polymer, is assumed to be ideally represented by a cohesive force model with a constant cohesive stress $\sigma = \sigma_{\mathrm{c}}$ for $0 \leqq \delta \leqq \delta_{\mathrm{c}}$ where δ is the opening displacement of bridging polymer and δ_{c} is its critical value, as shown in Fig. 6.

When the size of matrix crack bridging is of l_{c} in width, the apparent crack tip stress intensity factor due to the matrix crack bridging is given for a plane problem of rectilinearly anisotropic elasticity [13] by

$$K_{Ib}^{*} = -4(1 - V_{\mathrm{f}})\sigma_{\mathrm{c}}\sqrt{\frac{l_{\mathrm{c}}}{2\pi}}. \tag{13}$$

If the matrix crack bridging is restricted to be of small size ahead of the macroscopic stress-corrosion crack tip, the relationship between the critical value of the opening displacement of bridging polymer δ_{c} and the width of matrix crack bridging l_{c} is written as

$$\delta_{\mathrm{c}} = 4\Phi K_{\mathrm{I}}^{*}\sqrt{\frac{l_{\mathrm{c}}}{2\pi}} \tag{14}$$

where

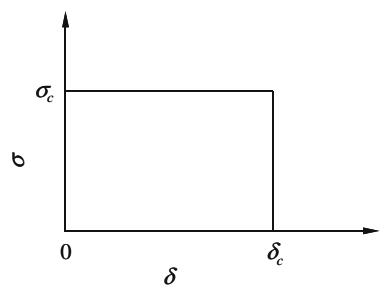

Fig. 6 Cohesive force model of bridging polymer

$$\Phi = \sqrt{b_{22}\{2(b_{11}b_{22})^{1/2} + 2b_{12} + b_{66}\}}. \tag{15}$$

In Eq. 15, b_{11}, b_{12}, b_{22} and b_{66} are constants which relate to the macroscopic elastic constants of the unidirectional GFRP, and are expressed as follows: in a plane stress condition,

$$b_{11} = \frac{1}{E_{\mathrm{T}}}, \quad b_{12} = -\frac{\nu_{\mathrm{LT}}}{E_{\mathrm{L}}}, \quad b_{22} = \frac{1}{E_{\mathrm{L}}}, \quad b_{66} = \frac{1}{G_{\mathrm{LT}}} \tag{16}$$

and in a plane strain condition,

$$b_{11} = \frac{1 - \nu_{\mathrm{TT}}^2}{E_{\mathrm{T}}}, \quad b_{12} = -\frac{\nu_{\mathrm{LT}}(1 + \nu_{\mathrm{TT}})}{E_{\mathrm{L}}}, \quad b_{22} = \frac{1 - E_{\mathrm{T}}\nu_{\mathrm{LT}}^2/E_{\mathrm{L}}}{E_{\mathrm{L}}}, \quad b_{66} = \frac{1}{G_{\mathrm{LT}}} \tag{17}$$

where E_{L} and E_{T} are the Young's moduli in the longitudinal and transverse directions, respectively, ν_{LT} and ν_{TT} are the Poisson's ratios for transverse strain under applied loads in the longitudinal and transverse directions, respectively, and G_{LT} is the shear modulus.

Substituting Eq. 13 into Eq. 12 and eliminating l_{c} by use of Eq. 14, we obtain

$$K_{\mathrm{I}}^{*} = \frac{K_{Ia}^{*} + \sqrt{K_{Ia}^{*\,2} - 4(1 - V_{\mathrm{f}})\sigma_{\mathrm{c}}\delta_{\mathrm{c}}/\Phi}}{2} \tag{18}$$

where

$$K_{Ia}^{*} \geqq 2\sqrt{(1 - V_{\mathrm{f}})\sigma_{\mathrm{c}}\delta_{\mathrm{c}}/\Phi}. \tag{19}$$

Meanwhile, geometrical consideration of the area of the stress-corrosion crack as shown in Fig. 3 gives the formula [9]:

$$\frac{\mathrm{d}Y}{\mathrm{d}t} = 4r_{\mathrm{f}}^{2}\sin^{2}\theta\frac{\mathrm{d}\theta}{\mathrm{d}t}. \tag{20}$$

Substituting Eq. 20 into Eq. 2 and using Eqs. 3 and 10, we obtain

$$\mathrm{d}t = \frac{2r_{\mathrm{f}}}{\nu k}\frac{\sin^{2}\theta}{\theta}\exp\left(-\frac{\alpha\beta F(\theta)\sqrt{2\pi r_{\mathrm{f}}}}{RT}K_{\mathrm{I}}^{*}\right)\mathrm{d}\theta \tag{21}$$

where

$$k = \exp\left(-\frac{\Delta Q}{RT}\right). \tag{22}$$

By integrating Eq. 21, the time required to propagate the stress-corrosion crack stably in the single glass fibre, t_{F}, is given by

$$t_F = \frac{2r_f}{vk}\int_{\theta_0}^{\theta_F}\frac{\sin^2\theta}{\theta}\exp\left(-\frac{\alpha\beta F(\theta)\sqrt{2\pi r_f}}{RT}K_I^*\right)d\theta \quad (23)$$

where θ_0 is half the angle made by two fibre radii on the edges of the inherent surface flaw and θ_F is that of the stress-corrosion crack at the onset of unstable fracture of the glass fibre. The unstable fracture of the glass fibre takes place when the crack tip stress intensity factor K_I attains the fracture toughness of glass K_{Ic}. By combining Eqs. 3 and 10, θ_F is therefore given by

$$\theta_F = F^{-1}\left(\frac{K_{Ic}}{\beta K_I^*\sqrt{2\pi r_f}}\right) \quad (24)$$

where F^{-1} is the inverse function of F given by Eq. 4.

The time required to the unstable fracture of the glass fibre is much shorter than the time t_F given by Eq. 23. Thus, the macroscopic crack growth rate da^*/dt is approximately given by

$$\frac{da^*}{dt} = \frac{D}{t_F}. \quad (25)$$

By introducing the following quantities [9]:

$$\zeta = \frac{vkD}{2r_f}, \quad \mu = \frac{\alpha\beta\sqrt{2\pi r_f}}{RT} \quad (26)$$

Substitution of Eq. 23 into Eq. 25 gives

$$\frac{da^*}{dt} = \frac{\zeta}{I} \quad (27)$$

where

$$I = \int_{\theta_0}^{\theta_F}\frac{\sin^2\theta}{\theta}\exp\{-\mu K_I^* F(\theta)\}\,d\theta. \quad (28)$$

Consider the integrand in the integral of Eq. 28. By taking account of the values of $\alpha = 0.110 \sim 0.216$ m$^{5/2}$/mol [10], $E_f = 68 \sim 87$ GPa, $E_m = 2.9 \sim 4.8$ GPa, $V_f = 0.40 \sim 0.57$, $R = 8.31$ J/(mol K) and $T = 298$ K at room temperature, the value of μ is estimated as

$$\mu = 96.6 \sim 295(\text{MPa m}^{1/2})^{-1}. \quad (29)$$

With regard to the apparent crack tip stress intensity factor K_I^*, its range has been set between 2 and 26 MPa m$^{1/2}$ in the previous experiments. Therefore, the integrand tends to zero, except for very small value of θ. By taking account of this fact, Eq. 28 is given approximately by the formula [9]:

$$I \approx \frac{4}{1.58\mu K_I^*}\left(\frac{1}{1.58\mu K_I^*}+\frac{\theta_0}{2}\right)\exp(-0.79\mu\theta_0 K_I^*). \quad (30)$$

Table 1 shows the approximate values calculated from Eq. 30 together with the exact values of I for a unidirectional GFRP with face-centred hexagonal array of fibre. The values of the Young's moduli of glass fibre and matrix, E_f, E_m, and the volume fraction of glass fibre V_f are taken, for instance, as E_f = 72.5 GPa, E_m = 4.0 GPa and V_f = 0.5, respectively. The apparent crack tip stress intensity factor K_I^* is fixed as 5 MPa m$^{1/2}$. For the fracture toughness of glass K_{Ic}, we use 0.73 MPa m$^{1/2}$ which corresponds to fracture energy γ_c = 3.7 J/m^2 for SiO_2 glass [14]. Then, the angle θ_F calculated from Eq. 24 is 4.29° (7.49×10^{-2} rad). It is recognised from Table 1 that the approximate value agrees to the exact value of I with satisfactory accuracy for $\theta_0 \leqq 2.5°$ (4.36×10^{-2} rad). Bartenev [15] pointed out that the depth of the pre-existing inherent surface flaw generated during the drawing of a commercial glass fibre of 10 μm diameter is less than 0.01 μm. For this depth, the angle θ_0 can be roughly estimated at less than 2.5°.

Substituting Eq. 30 into Eq. 27, we obtain the macroscopic crack growth rate da^*/dt in the unidirectional GFRP as follows:

Table 1 Values of I

θ_0	μ = 150 (MPa m$^{1/2}$)$^{-1}$			μ = 250 (MPa m$^{1/2}$)$^{-1}$		
	Approximate	Exact	Error (%)	Approximate	Exact	Error (%)
0.2°	1.1048×10^{-6}	1.0958×10^{-6}	0.8	1.4520×10^{-7}	1.4356×10^{-7}	1.1
0.4°	2.3381×10^{-7}	2.3091×10^{-7}	1.3	8.2069×10^{-9}	8.0521×10^{-9}	1.9
0.6°	4.1456×10^{-8}	4.0783×10^{-8}	1.7	3.7541×10^{-10}	3.6580×10^{-10}	2.6
0.8°	6.7450×10^{-9}	6.6146×10^{-9}	2.0	1.5586×10^{-11}	1.5102×10^{-11}	3.2
1.0°	1.0428×10^{-9}	1.0205×10^{-9}	2.2	6.1195×10^{-13}	5.9056×10^{-13}	3.6
1.5°	8.6259×10^{-12}	8.4477×10^{-12}	2.1	1.6302×10^{-16}	1.5730×10^{-16}	3.6
2.0°	6.4355×10^{-14}	6.3813×10^{-14}	0.8	3.8954×10^{-20}	3.8306×10^{-20}	1.7
2.5°	4.5282×10^{-16}	4.6162×10^{-16}	−1.9	8.7588×10^{-24}	9.0002×10^{-24}	−2.7
3.0°	3.0681×10^{-18}	3.2768×10^{-18}	−6.4	1.8942×10^{-27}	2.0979×10^{-27}	−9.7

$$\frac{da^*}{dt} = 1.25\zeta\mu^2 K_I^{*2}\left(\frac{1}{2+1.58\mu\theta_0 K_I^*}\right)\exp(0.79\mu\theta_0 K_I^*). \quad (31)$$

By recalling Eq. 18, Eq. 31 yields the relationship between the macroscopic crack growth rate da^*/dt and the apparent crack tip stress intensity factor due to an applied load K_{Ia}^*. It is worthwhile noting from Eq. 31 that the macroscopic crack growth rate is independent of the radius and the fracture toughness of glass fibre.

In a plane strain condition, the relationship is shown in a logarithmic plot for various values of θ_0 and δ_c in Fig. 7. The values of ζ and μ are set, for instance, as $\zeta = 5 \times 10^{-15}$ m/s and $\mu = 115$ (MPa m$^{1/2}$)$^{-1}$. The cohesive stress of bridging polymer is taken as $\sigma_c = 80$ MPa. The values of macroscopic elastic constants of a unidirectional GFRP and volume fraction of glass fibre are tabulated in Table 2. As can be seen from the figure, the macroscopic crack growth rate da^*/dt increases with the apparent crack tip stress intensity factor K_{Ia}^*. Moreover, the larger the size of inherent surface flaw of glass fibre, the higher the macroscopic crack growth rate. The figure also reveals that the macroscopic crack growth rate is even lower with decreasing the apparent crack tip stress intensity factor due to an applied load because the effect of matrix crack bridging is more pronounced at a low value of K_{Ia}^*.

It can be also seen in Fig. 7 that there exists the lowest limit of the apparent crack tip stress intensity factor K_{Ia}^* for the macroscopic stress-corrosion crack to propagate, unless $\delta_c = 0$. The lowest limit is marked by an arrow in Fig. 7. The lowest limit shifts to a higher value of the apparent crack tip stress intensity factor K_{Ia}^* as the critical value of the opening displacement of bridging polymer becomes larger. Friedrich [5] and Aveston and Sillwood [6] observed some evidence of a stress-corrosion limit by the experiment. Although the physical implication of the lowest limit is that breakage of bridging polymer does not take place at the macroscopic stress-corrosion crack tip below the limit, the lowest limit should be understood as the threshold stress intensity factor for stress-corrosion cracking K_{Iscc}^*, which is given through Eq. 19 with the equality by

$$K_{Iscc}^* = 2\sqrt{(1-V_f)\sigma_c\delta_c/\Phi}. \quad (32)$$

Table 2 Values of macroscopic elastic constants of a unidirectional GFRP and volume fraction of glass fibre

$E_L = 44.1$ GPa, $E_T = 9.65$ GPa
$\nu_{LT} = 0.28$, $\nu_{TT} = 0.23$
$G_{LT} = 4.13$ GPa
$V_f = 0.55$

Discussion

There is experimental data in the literature [6] on a unidirectional GFRP containing E-glass fibres of $V_f = 0.50$ in an orthophthalic polyester resin matrix. Stress-corrosion crack propagation tests were carried out in 1 N sulphuric acid at room temperature under a static load. Figure 8 shows a logarithmic plot of the data of macroscopic crack growth rate against the apparent crack tip stress intensity factor due to an

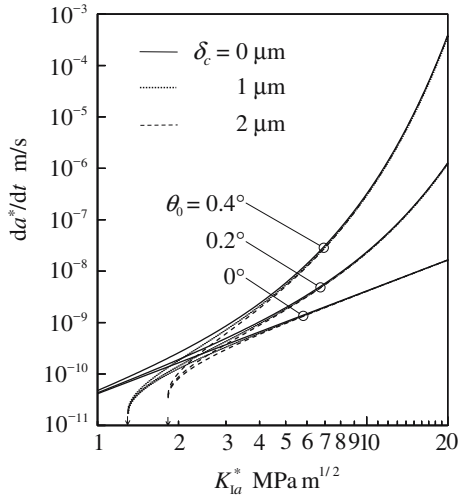

Fig. 7 Macroscopic crack growth rate versus apparent crack tip stress intensity factor due to an applied load

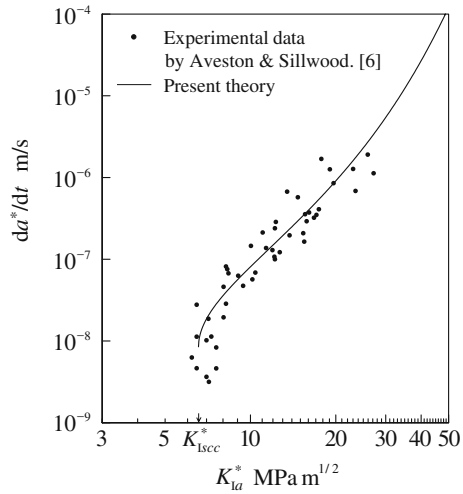

Fig. 8 Comparison between experimental and theoretical results of macroscopic crack growth rate

Table 3 Values of power in simple power law

Material	Environment	Value of power	Reference
Unidirectional E-glass/polyester	0.6 N HCl	3.57, 4.22	3
		2.56, 2.73, 3.99, 5.3	4
Unidirectional E-glass/polyester	1 N H_2SO_4	3.1	6

applied load K^*_{Ia}. Comparison between experiment and theory can be made by calculating da^*/dt for the values of $\zeta = 8.5 \times 10^{-14}$ m/s, $\mu = 118$ (MPa $m^{1/2})^{-1}$, $\theta_0 = 0.076°$, $\sigma_c\delta_c = 1.85$ kPa m and $\Phi = 8.60 \times 10^{-2}$ $(GPa)^{-1}$. The theoretical result of macroscopic crack growth rate is shown by the solid line in Fig. 8, and is in good agreement with experimental measurement. This gives confidence in the physical model.

In the case where $\theta_0 = 0°$ and $\delta_c = 0$, referring to Eqs. 18 and 31 the relationship between the macroscopic crack growth rate da^*/dt and the apparent crack tip stress intensity factor due to an applied load K^*_{Ia} reduces simply to

$$\frac{da^*}{dt} = 0.625\zeta\mu^2 K^{*\,2}_{Ia}. \tag{33}$$

This formula demonstrates that the variation of da^*/dt with K^*_{Ia} obeys the simple power law to the power of two.

As can be seen from Fig. 7, if the apparent crack tip stress intensity factor is experimentally set over a small range, $\log(da^*/dt)$ is observed to be essentially linear with $\log K^*_{Ia}$. This means that the relationship between da^*/dt and K^*_{Ia} is represented by a simple power law of the form:

$$\frac{da^*}{dt} = AK^{*\,m}_{Ia} \tag{34}$$

where m and A are constants. Figure 7 also shows that the power of two is the smallest power over a small range of K^*_{Ia}.

Table 3 gives the values of power for a unidirectional GFRP, which are obtained experimentally in the previous studies. We can see that all values of power are larger than two. As a consequence, the experimental results of the previous studies are consistent with the result that the smallest power is two.

Conclusions

A physically based micro-mechanical theory of macroscopic stress-corrosion cracking in a unidirectional GFRP has been presented. The effect of matrix crack bridging on the macroscopic crack growth rate has been included in the theory. We have derived an equation which represents the relationship between the macroscopic crack growth rate and the apparent crack tip stress intensity factor due to an applied load. The relationship has been depicted in the figure. We have found from the figure that the macroscopic crack growth rate becomes lower by reducing the size of inherent surface flaw of glass fibre and by the matrix crack bridging in the crack wake. Moreover, there exists the lowest limit of the apparent crack tip stress intensity factor in the presence of the matrix crack bridging. This threshold stress intensity factor shifts to a higher value of the apparent crack tip stress intensity factor as the critical value of the opening displacement of bridging polymer becomes larger. For the limiting case, where the glass fibre is free of inherent surface flaws and the matrix crack bridging is negligible, the relationship is represented by a simple power law to the power of two.

References

1. Hogg PJ, Hull D (1980) Met Sci 14:441
2. Noble B, Harris SJ, Owen MJ (1983) J Mater Sci 18:1244
3. Price JN, Hull D (1983) J Mater Sci 18:2798
4. Price JN, Hull D (1987) Compos Sci Tech 28:193
5. Friedrich K (1981) J Mater Sci 16:3292
6. Aveston J, Sillwood JM (1982) J Mater Sci 17:3941
7. Hsu P-L, Yau S-S, Chou T-W (1986) J Mater Sci 21:3703
8. Sekine H, Miyanaga T (1990) J Soc Mater Sci, Japan 39:1545
9. Sekine H, Beaumont PWR (1998) Compos Sci Tech 58:1659
10. Wiederhorn SM, Bolz LH (1970) J Am Ceram Soc 53:543
11. Sekine H, Hu N, Fukunaga H (1995) Compos Sci Tech 53:317
12. Kiuchi A, Aoki M, Kobayashi M, Ikeda K (1982) J Iron Steel Inst Japan 68:1830
13. Sih GC, Paris PC, Irwin GR (1965) Int J Fract Mech 1:189
14. Mecholsky JJ, Rice RW, Freiman SW (1974) J Am Ceram Soc 57:440
15. Bartenev GM (1969) Int J Fract Mech 5:179